NASA/TM—2006-214096

Composite Erosion by Computational Simulation

Christos C. Chamis
Glenn Research Center, Cleveland, Ohio

February 2006

NASA STI Program . . . in Profile

Since its founding, NASA has been dedicated to the advancement of aeronautics and space science. The NASA Scientific and Technical Information (STI) program plays a key part in helping NASA maintain this important role.

The NASA STI Program operates under the auspices of the Agency Chief Information Officer. It collects, organizes, provides for archiving, and disseminates NASA's STI. The NASA STI program provides access to the NASA Aeronautics and Space Database and its public interface, the NASA Technical Reports Server, thus providing one of the largest collections of aeronautical and space science STI in the world. Results are published in both non-NASA channels and by NASA in the NASA STI Report Series, which includes the following report types:

- TECHNICAL PUBLICATION. Reports of completed research or a major significant phase of research that present the results of NASA programs and include extensive data or theoretical analysis. Includes compilations of significant scientific and technical data and information deemed to be of continuing reference value. NASA counterpart of peer-reviewed formal professional papers but has less stringent limitations on manuscript length and extent of graphic presentations.

- TECHNICAL MEMORANDUM. Scientific and technical findings that are preliminary or of specialized interest, e.g., quick release reports, working papers, and bibliographies that contain minimal annotation. Does not contain extensive analysis.

- CONTRACTOR REPORT. Scientific and technical findings by NASA-sponsored contractors and grantees.

- CONFERENCE PUBLICATION. Collected papers from scientific and technical conferences, symposia, seminars, or other meetings sponsored or cosponsored by NASA.

- SPECIAL PUBLICATION. Scientific, technical, or historical information from NASA programs, projects, and missions, often concerned with subjects having substantial public interest.

- TECHNICAL TRANSLATION. English-language translations of foreign scientific and technical material pertinent to NASA's mission.

Specialized services also include creating custom thesauri, building customized databases, organizing and publishing research results.

For more information about the NASA STI program, see the following:

- Access the NASA STI program home page at *http://www.sti.nasa.gov*

- E-mail your question via the Internet to *help@sti.nasa.gov*

- Fax your question to the NASA STI Help Desk at 301–621–0134

- Telephone the NASA STI Help Desk at 301–621–0390

- Write to:
  NASA STI Help Desk
  NASA Center for AeroSpace Information
  7121 Standard Drive
  Hanover, MD 21076–1320

NASA/TM—2006-214096

Composite Erosion by Computational Simulation

Christos C. Chamis
Glenn Research Center, Cleveland, Ohio

Prepared for the
SAMPE 2006
sponsored by the Society for the Advancement of Material and Process Engineering
Long Beach, California, April 30–May 4, 2006

National Aeronautics and
Space Administration

Glenn Research Center
Cleveland, Ohio 44135

February 2006

Level of Review: This material has been technically reviewed by technical management.

Available from

NASA Center for Aerospace Information
7121 Standard Drive
Hanover, MD 21076–1320

National Technical Information Service
5285 Port Royal Road
Springfield, VA 22161

Available electronically at http://gltrs.grc.nasa.gov

Composite Erosion by Computational Simulation

Christos C. Chamis
National Aeronautics and Space Administration
Glenn Research Center
Cleveland, Ohio 44135

Abstract

Composite degradation is evaluated by computational simulation when the erosion degradation occurs on a ply-by-ply basis and the degrading medium (device) is normal to the ply. The computational simulation is performed by a multi factor interaction model and by a multi scale and multi physics available computer code. The erosion process degrades both the fiber and the matrix simultaneously in the same slice (ply). Both the fiber volume ratio and the matrix volume ratio approach zero while the void volume ratio increases as the ply degrades. The multi factor interaction model simulates the erosion degradation, provided that the exponents and factor ratios are selected judiciously. Results obtained by the computational composite mechanics show that most composite characterization properties degrade monotonically and approach "zero" as the ply degrades completely.

1. Introduction

Composites erosion is an important design requirement when composite structures are subjected to erosion environments. A significant amount of research has been and continues to be conducted on that subject. Some of that research is summarized in references 1 and 2. Reference 1 covers research up to 1986. This is a multi author publication by specialists in all aspects of erosion. Reference 2 is another multi author publication that covers tribology research up to 1993. This publication also covers various aspects of tribology research that has been performed through August of 1992. These two publications provide a very good orientation for beginners in composites erosion and some of the concepts described in the present article. Specific aspects of erosion in injection moulded thermoplastic composites are described in reference 3. The main feature in this reference is that erosion occurs on a composite slice (ply) at the time. Friction and wear of several polymer composites are investigated experimentally in reference 4. The main finding in that investigation is that the friction coefficient remains constant and does depend on which surface the eroding device is acting. They found that for the various laminates that they tested the coefficient of friction was about the same. They also found that the prodding mass depends on the pressure exerted by the eroding device on the eroding surface. Barkoula and Karger-Kocsis performed solid particle tests (ref. 5) on composites with different fiber/matrix adhesion. They found that improvements in the interface bond reduce substantially the eroded mass for the same testing conditions. The only simulation that was found is that for thermal analysis by finite element for the heat transfer in sliding friction (ref. 6). They found that the finite element can be used in that sliding situation. An ASME publication (ref. 7) describes micro and nano tribology. This publication deals mainly with chemistry at the nano scale. The articles that were reviewed do not deal with the composite mechanics simulation of the composite erosion and the composite properties as the erosion proceeds. It became obvious to the author that an investigation that utilizes simulation of the composite erosion was needed. Therefore, the objective of the present investigation is to use computational composite mechanics in order to evaluate composite erosion and the respective composite degradation in terms of its degraded properties. Specifically, the application of available computational methods ICAN (ref. 8) to evaluate composite degradation due to erosion. The other computational simulation method used was the Multi Factor Interaction Model (MFIM) which can be used to simulate composite erosion when the exponents of each factor and their respective ratios are chosen judiciously. The erosion considered is that as the erosion progresses as the fiber volume ratio the matrix volume ratio and the fiber diameter decrease simultaneously. The properties predicted then will be as each slice in a ply degrades due to the changes in those variables.

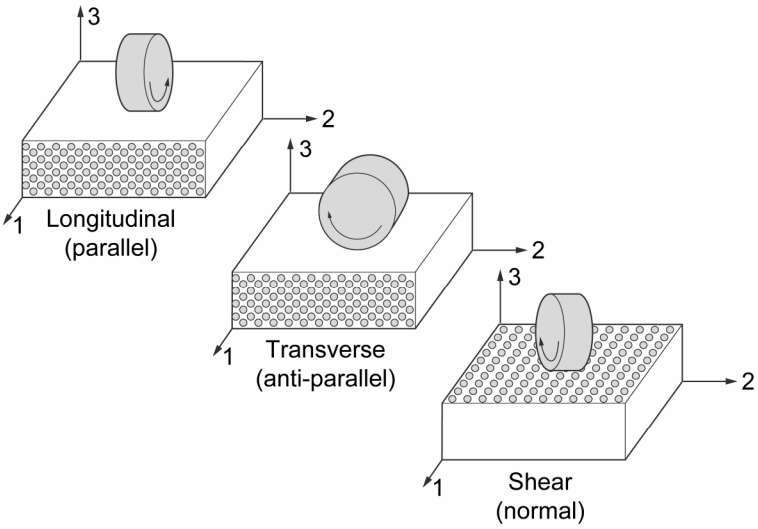

Figure 1.—Three modes of erosion.

2. Fundamentals of Erosion

In this section we consider the fundamental modes of erosion which are illustrated in figure 1. As can be seen in that figure, there are three modes of erosion which are taken to be consistent with those of mechanical stress. The reason for this is that subsequent transformation of erosion will follow that of the stress tensor. It is assumed that the longitudinal (erosion parallel to the fibers) will be the most resistant to the eroding stress because the stiffness of the fibers is the greatest in that direction (fig. 1(a)). The second mode of erosion is transverse to the fiber direction (fig. 1(b)). In this case, the fiber stiffness is about an order of magnitude lower than the longitudinal and, therefore, the erosion will be about an order of magnitude higher than the longitudinal (fig. 1(b)). The third mode of erosion is that due to shear stress as depicted in figure 1(c). The resistance to erosion in this mode will be about proportional to the shear stiffness of the laminate which is approaching two orders of magnitude lower than the longitudinal stiffness. In this case, the erosion resistance will be about two orders of magnitude higher than the longitudinal. The magnitude of the eroding stress depends on the applied normal force to that plane and the plane's respective coefficient of friction. Data shows that the coefficient of friction is the same for all three modes (1). Therefore, the eroding stress will depend on the force that is acting on that surface and the stress developed there from.

3. Coefficient of Friction

It would be meaningful to have a coefficient of friction which is a function of the constituents in the composite. Considering the fact (1) that the coefficient of friction is not direction dependent and it does depend on the fiber volume ratio. Then a coefficient of friction can be determined by assuming that the eroding force will strain and, therefore, erode fibers and the matrix in the same amount and create voids as well. The coefficient of friction (μ) is generally defined as:

$$\mu = \frac{F_n}{A} \tag{1}$$

where F_n represents the force normal to the surface and A is the area on which the force acts. The area includes both the fiber and the matrix and any voids that may be present or created as a result of the erosion process. Now, assuming an area of unit thickness (t) we have the volume is equal

$$V = At = A_f t + A_m t + A_v t \tag{2}$$

where the subscripts *f*, *m*, and *v* denote fiber, matrix and voids respectively.

Dividing through by *t* we obtain

$$A = A_f + A_m + A_v \tag{3}$$

Divide through by *A*

$$1 = \frac{A_f}{A} + \frac{A_m}{A} + \frac{A_v}{A} \tag{4}$$

Let $A_f/A = k_f$; $A_m/A = k_m$, and $A_v/A = k_v$, we obtain the following result:

$$1 = k_t + k_m + k_v \tag{5}$$

Since the strain is constant due to eroding device, then the local stresses are proportional to the local stiffness.

$$\sigma_{f11} = A_f E_{f11} e;\ \sigma_{m1} = A_m E_m e;\ \sigma_v = A_v E_v e = o;\ (E_v = o) \tag{6}$$

The force on the eroding surface is

$$F = A_f \sigma_{f11} + A_m \sigma_{m11} = F_n \mu_c = N_{zz} \tag{7}$$

Noting that the friction coefficient has the same units as the modules, and making the equivalent substitution and neglecting the void term, we obtain the equation for the friction coefficient:

$$\frac{1}{\mu_c} = \frac{k_f}{\mu_f} + \frac{k_m}{\mu_m} \tag{8}$$

This equation is the same as that in reference 1. Rearranging equation (8) yields:

$$\frac{1}{\mu_c} = \frac{\mu_m k_f + \mu_f k_m}{\mu_f \mu_m} \tag{9}$$

$$\mu_c = \frac{\mu_f \mu_m}{\mu_m k_f + \mu_f k_m} \tag{10}$$

Upon dividing by μ_f

$$\mu_c = \frac{\mu_m}{\frac{\mu_m}{\mu_f} k_f + k_m} = \frac{\mu_m}{k_m + k_f \left(\frac{\mu_m}{\mu_f} \right)} \tag{11}$$

Equation (11) shows that for constant k_m and (μ_m/μ_f), μ_c will decrease as k_f increases which is an interesting result.

4. Composite Wear Due To Erosion

Composites will erode if there is an erosive device which degrades the composites. Experimental data shows that the wear volume in an eroded composite is a function of several quantities as shown below (1):

$$Q = f\left(V, \mu_c, E, S_{\ell 12S}, N_{zz}, k_f\right) \tag{12}$$

Where Q is the eroded volume, V is the eroding device velocity, μ_c is the composite friction coefficient, $S_{\ell 12S}$ is the composite shear strength, N_{zz} is the normal load, $E = E_c$ is the composite modulus normal to the eroding plane, and k_f is the fiber volume fraction in the composite. That volume of the erosion includes (1) wear or fiber thinning, (2) matrix thinning or gauging that will cause fiber breaks or fiber peeling. Two methods of solution will be pursued. (1) is the multi factor interaction model, and (2) a heuristic method based on the physics of the problem.

5. Erosion Simulation by the MFIM

We can now express the degraded volume by applying the multi factor interaction module in expanded form.

$$\frac{Q_c}{Q_i} = \left(1 - \frac{V}{V_i}\right)^{e_1}\left(1 - \frac{\mu_c}{\mu_{c\ell}}\right)^{e_2}\left(1 - \frac{N_{zz}}{N_{zzF}}\right)^{e_3}\left(1 - \frac{E_c}{E_{c\ell}}\right)^{e_4}\left(1 - \frac{S_{\ell 12}}{S_{\ell 12S}}\right)^{e_5}\left(1 - \frac{k_{f3}}{k_{fF}}\right)^{e_6} \tag{13}$$

One disadvantage of MFIM is the selection of the exponents, e_1 through e_6. A sample example of the difficulty is illustrated in figure 2 where the non-eroded composite thickness is plotted versus a constant value of mean ratio or a constant value of the exponents. In the first case the exponents are varying from 0.1 to 0.9 and in the second case the ratios vary from 0.1 to 0.9. The important observation in figure 2 is that the remaining thickness erodes a lot faster at the early part of the erosion process. The MFIM results

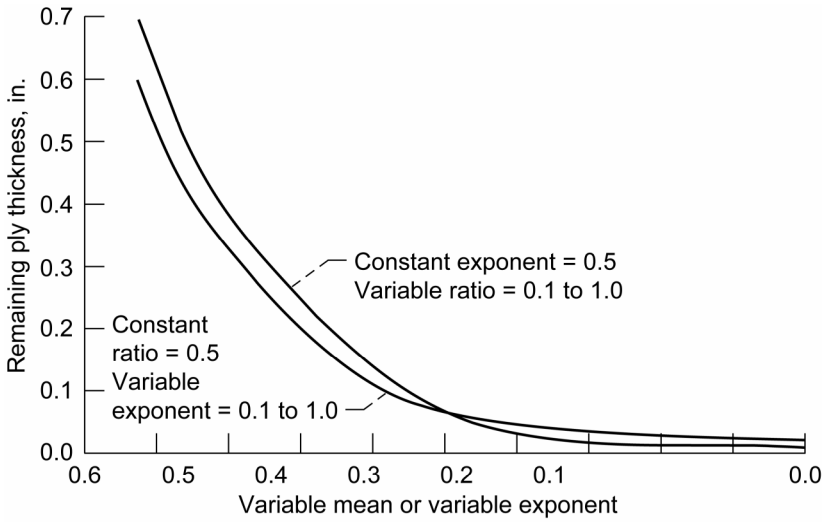

Figure 2.—Remaining ply thickness decreases rapidly with increases in mean ratio or exponent.

for assuming a constant value of all the exponents of 0.5 and/or variable mean ratio are summarized in table 1. It is seen in this table that the remaining thickness is $Q_c/Q_i = 0.0085$, which is very low. The sensitivities with respect to the remaining thickness are summarized in the last column of this table. Another example is one with varying exponents and ratios simultaneously. The results are summarized in table 2. It can be seen that the ratio value $Q_c/Q_i = 0.0026$. Apparently a multitude of eroded values are obtainable by using the MFIM. Another example of the inclusiveness of MFIM is summarized in table 3. As can be seen, the ratio value $Q_c/Q_i = 0.9906$. The corresponding sensitivities are listed in the last column of that table. Experimental values range from 0 to 0.005 μm for normal erosion versus time (ref. 1). Using this as an anchoring point, the value obtained in table 3 of 0.996 is compared to 0.024. The 0.024 value can be readily obtained with some manipulation of the exponents and the ratios in the MFIM. The interesting point to be made is that the MFIM has many degrees of freedom which permit simulation of any measured data irrespective of how the data was obtained.

TABLE 1

Term	Exponent	Factor Ratio	Relative to Q_c
1	0.5	0.8	–0.0212
2	0.5	0.9	–0.0424
3	0.5	0.5	–0.0085
4	0.5	0.8	–0.0212
5	0.5	0.9	–0.0424
6	0.5	0.6	–0.0106
7	0.5	0.1	–0.0047
Note: $Q_c/Q_i = 0.0085$			

TABLE 2

Term	Exponent	Factor Ratio	Relative to Q_c
1	0.6	0.8	–0.0212
2	0.8	0.9	–0.0424
3	0.5	0.5	–0.0085
4	0.4	0.8	–0.0212
5	0.7	0.9	–0.0424
6	0.5	0.6	–0.0106
7	0.9	0.1	–0.0047
Note: $Q_c/Q_i = 0.0026$			

TABLE 3

Term	Exponent	Factor Ratio	Relative to Q_c
1	–0.6	0.8	2.9719
2	0.8	0.9	–7.9251
3	–0.5	0.5	0.9906
4	0.4	0.8	–1.9813
5	–0.7	0.9	6.9345
6	0.5	0.6	–1.2383
7	–0.1	0.1	0.1101
Note: $Q_c/Q_i = 0.996$			

6. Simulation by Computational Composite Mechanics

The simulation of the composite erosion by using computational composite mechanics is based on the following assumption: “The eroded composite will occur on a ply-per-ply basis where the eroding device degrades equal thickness of fiber and matrix.” What is needed then is to simulate the erosion degradation in the exposed ply first. Once this is done the erosion in subsequent places in the laminate can be accomplished by following the same procedure that was for simulating the erosion degradation in the exposed ply. The procedure to be described below is based on having available a computational composite mechanics code whose micromechanics are based on constituent materials and fiber diameter,

fiber, matrix, and void volume ratios. The constituent properties for the simulation are listed in table 4 for fiber and in table 5 for matrix. The results described below are for all the composite properties of a uniaxial ply as it erodes from its pristine conditions to its end. The erosion is assumed to progress as the eroding device erodes the fibers and the matrix in the plan as was described previously.

TABLE 4. AS-4 GRAPHITE FIBER PROPERTIES

Number of fibers per end	Nf	10000	number
Filament equivalent diameter	df	0.300E-03	inches
Weight density	Rhof	0.630E-01	lb/in**3
Normal moduli (11)	Ef11	0.329E+08	psi
Normal moduli (22)	Ef22	0.199E+07	psi
Poisson's ratio (12)	Nuf12	0.200E+00	non-dim
Poisson's ratio (23)	Nuf23	0.250E+00	non-dim
Shear moduli (12)	Gf12	0.200E+07	psi
Shear moduli (23)	Gf23	0.100E+07	psi
Thermal expansion coef. (11)	Alfaf11	–0.550E-06	in/in/F
Thermal expansion coef. (22)	Alfaf22	0.560E-05	in/in/F
Heat conductivity (11) in/hr/in**2/F	Kf11	0.403E+01	BTU-
Heat conductivity (22) in/hr/in**2/F	Kf22	0.403E+00	BTU-
Heat capacity	Cf	0.170E+00	BTU/lb/F
Fiber tensile strength	SfT	0.430E+06	psi
Fiber compressive strength	SfC	0.430E+06	psi

TABLE 5. INTERMEDIATE MODULU AND STRENGTH EPOXY MATRIX

Weight density	Rhom	0.440E-01	lb/in**3
Normal modulus	Em	0.530E+06	psi
Poisson's ratio	Num	0.350E+00	non-dim
Thermal expansion coef.	Alfa m	0.360E-04	in/in/F
Matrix heat conductivity in/hr/in**2/F	Km	8.681E-03	BTU
Heat capacity	Cm	0.250E+00	BTU/lb/F
Matrix tensile strength	SmT	0.155E+05	psi
Matrix compressive strength	SmC	0.350E+05	psi
Matrix shear strength	SmS	0.130E+05	psi
Allowable tensile strain	eps mT	0.200E-01	in/in
Allowable compressive strain	eps mC	0.500E-01	in/in
Allowable shear strain	eps mS	0.350E-01	in/in
Allowable torsional strain	eps mTOR	0.350E-01	in/in
Void heat conductivity in/hr/in**2/F	kv	0.225E+00	BTU
Glass transition temperature	Tgdr	0.420E+03	F

(Scales: in = 25 mm; lb/in^3 = 6.41E-6 kg/m^3; E+6 psi = 6.8 GPa; E-6(in/in)/°F = 0.51E-6(cm/cm)/°C BTU-in/hr/in^2/°F = 0.07 J-in/hr/in^2/°C; BTU/lb/°F = 4.19E3J/kg/°C; ksi = 6.89 MPa; °F = 1.82 °C)

7. Erosion Effects on ply Configuration

The ply configuration geometric affects are summarized in figure 3. The ply thickness is defined as $t\ell$. The inter fiber distance is defined as $\delta\ell$. The ply fiber volume ratio is defined as k_f, the matrix as k_m and the void as k_v. These geometric properties are coded in the computer code ICAN (ref. 8). The erosion affects on the ply thickness is illustrated in figure 4. The ordinate in this figure shows the remaining ply thickness as the fiber volume ration decreases. It is observed in figure 4 that the thickness degrades linearly as the fiber volume ratio decreases. In figure 5 the remaining fiber diameter also decreases linearly as the fiber volume ratio decreases. The matrix volume ratio decreases nonlinearly as the fiber volume ratio decreases as shown in figure 6. The void volume ratio increases nonlinearly as the fiber volume ratio decreases, as shown in figure 7. It is interesting to note that the void volume ratio reaches about 1.0, indicating that both the volume fraction of the fiber and of the matrix have completely degraded. The inter fiber distance increases nonlinearly as the fiber volume ratio decreases as shown in figure 8. It is interesting to note in figure 8 that the inter fiber distance increases about five times as the ply approaches total degradation.

Partial volumes: $k_f + k_m + k_v = 1$

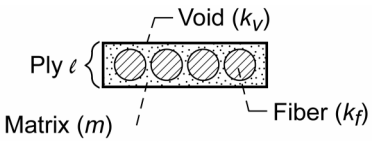

Ply density: $\rho_\ell = k_f \rho_f + k_m \rho_m$

Resin volume ratio: $k_m = (1 - k_v) / \left[1 + (\rho_m / \rho_f)(1/\lambda_m - 1)\right]$

Fiber volume ratio: $k_f = (1 - k_v) / \left[1 + (\rho_f / \rho_m)(1/\lambda_f - 1)\right]$

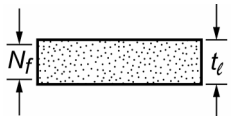

Weight ratios: $\lambda_f + \lambda_m = 1$

Ply thickness (S.A.): $t_\ell = 1/2\, N_f\, d_f \sqrt{\pi / k_f}$

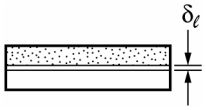

Interply thickness: $\delta_\ell = 1/2 \left[\sqrt{\pi / k_f} - 2\right] d_f$

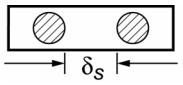

Inter fiber spacing (S.A.): $\delta_s = \delta_\ell$

Contiguous fibers (S.A.): $k_f = \pi/4 \sim 0.785$

Figure 3.—Micromechanics, geometric relationships.

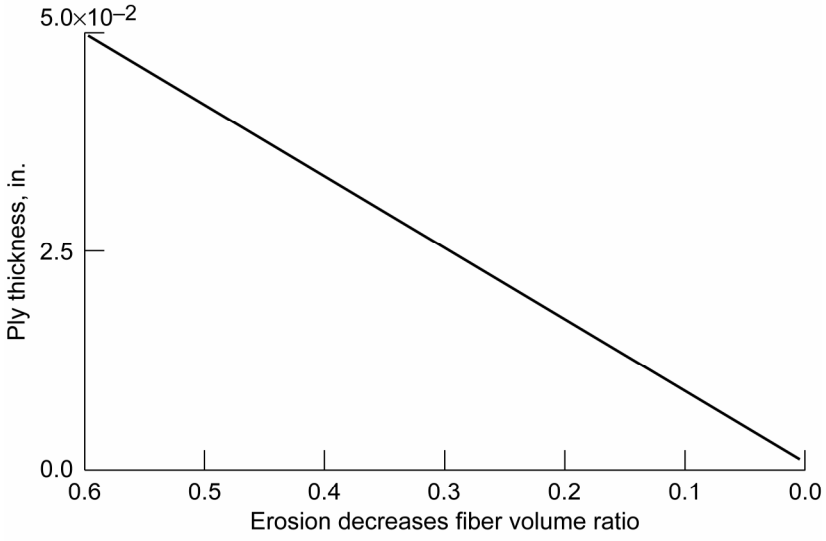

Figure 4.—Erosion effects on ply thickness ([0/±45/90_2/±45/0] as-graphite-fiber/intermediate modulus and strength matrix).

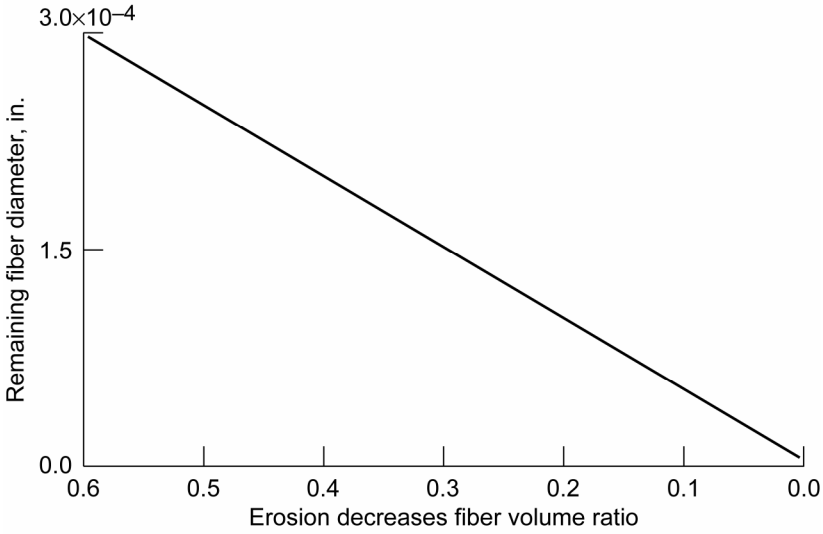

Figure 5.—Erosion effects on fiber diameter ([0/±45/90_2/±45/0] as-graphite-fiber/intermediate modulus and strength matrix). (in. = 25 mm).

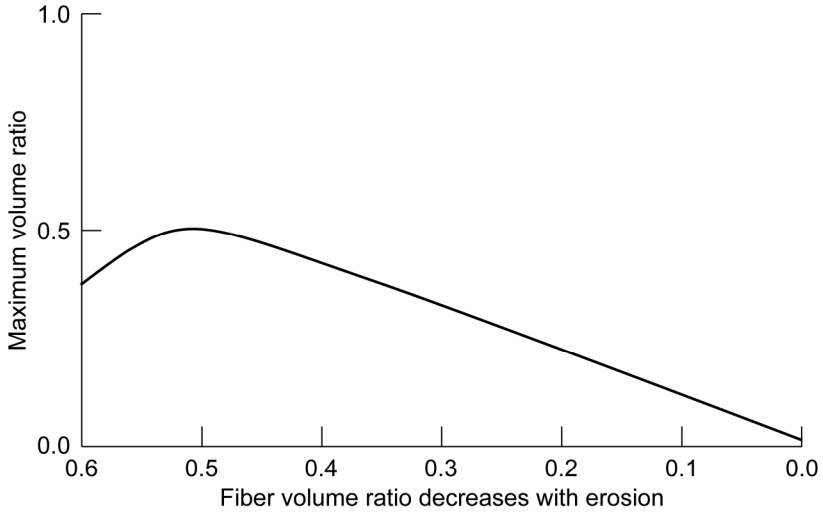

Figure 6.—Erosion effects on matrix volume ratio ([0/±45/90_2/±45/0] as-graphite-fiber/intermediate modulus and strength matrix).

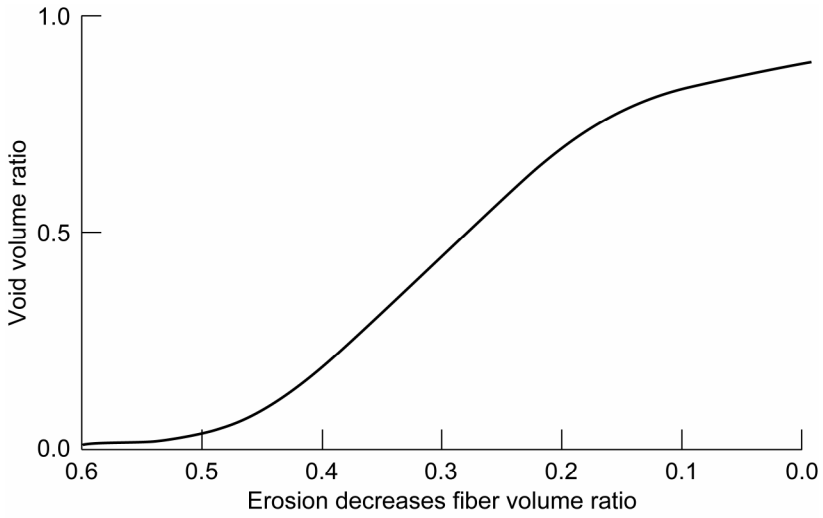

Figure 7.—Erosion effects on void volume ratio ([0/±45/90_2/±45/0] as-graphite-fiber/intermediate modulus and strength matrix).

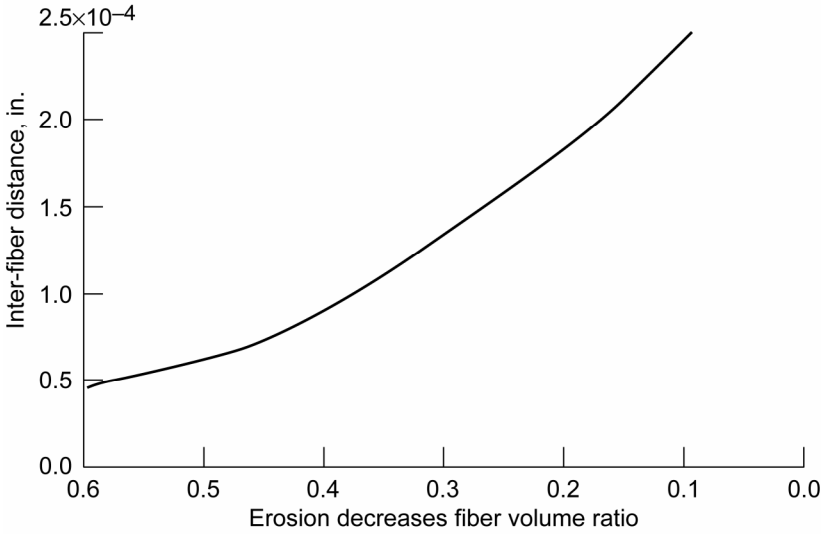

Figure 8.—Erosion effects on inter-fiber spacing ([0/±45/90_2/±45/0] as-graphite-fiber/intermediate modulus and strength matrix). (in. = 25 mm).

8. Thermal Properties Degradation

The micro mechanics equations that control thermal properties erosion degradation are summarized in figure 9. These equations are coded in the ICAN computer code. The ℓ subscript denotes ply property while the number subscripts denote directions. The ply longitudinal heat conductivity decreases linearly as the fiber volume ratio decreases as shown in figure 10. It is interesting to note in figure 10 that the longitudinal heat conductivity approaches “0” as the fiber volume ratio approaches zero. The ply transverse heat conductivity decreases initially nonlinearly, then levels off and remains insensitive to a decreasing fiber volume ratio as shown in figure 11. The thermal heat capacity remains relatively insensitive as the fiber volume ratio degrades as can be seen in figure 12. The erosion degraded thermal longitudinal expansion coefficient degrades nonlinearly with degraded fiber volume ratio as shown in

Heat capacity:

$$C_\ell = \frac{1}{\rho_\ell}\left(k_f\,\rho_f\,C_f + k_m\,\rho_m\,C_m\right)$$

Longitudinal conductivity:

$$K_{\ell 11} = k_f K_{f11} + k_m K_m$$

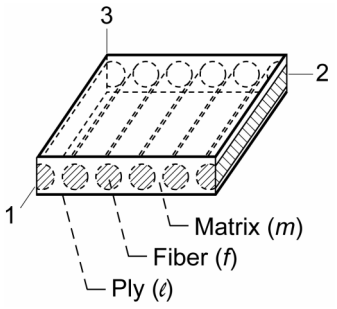

Transverse conductivity:

$$K_{\ell 22}\left(1-\sqrt{k_f}\right)K_m + \frac{K_m\sqrt{k_f}}{1-\sqrt{k_f}\left(1-K_m/K_{f22}\right)} = K_{\ell 33}$$

For voids:

$$K_m = \left(1-\sqrt{k_v}\right)K_m + \frac{K_m\sqrt{k_v}}{1-\sqrt{k_v}\left(1-K_m/K_v\right)}$$

Longitudinal thermal expansion coefficient:

$$\alpha_{\ell 11} = \frac{k_f\,\alpha_{f11}\,E_{f11} + k_m\,\alpha_m\,E_m}{E_{\ell 11}}$$

Transverse thermal expansion coefficient:

$$\alpha_{\ell 22} = \alpha_{f22}\sqrt{k_f} + \left(1-\sqrt{k_f}\right)\left(1+k_f\,\nu_m\,E_{f11}/E_{\ell 11}\right)\alpha_m = \alpha_{\ell 33}$$

Figure 9.—Composite micromechanics, thermal properties.

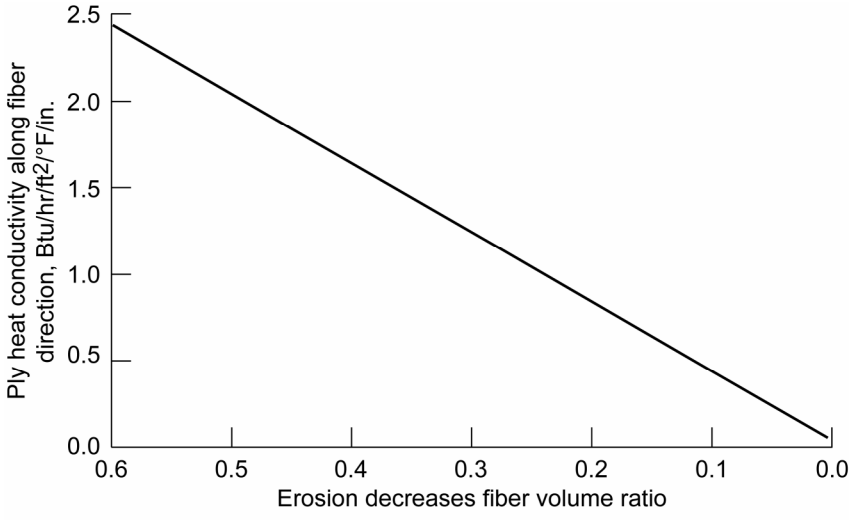

Figure 10.—Erosion effects on the longitudinal heat conductivity ([0/±45/90_2/±45/0] as-graphite-fiber/intermediate modulus and strength matrix). (Btu-in./hr/in.^{2}/°F = 0.07 J-m/hr/m^2/°C).

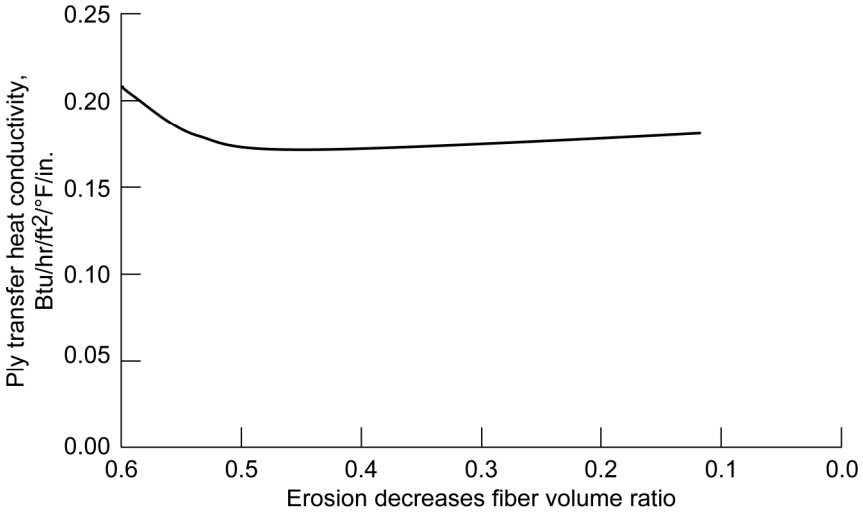

Figure 11.—Erosion effects on transverse heat conductivity ([0/±45/90_2/±45/0] as-graphite-fiber/intermediate modulus and strength matrix). (Btu-in./hr/$in.^2$/°F = 0.07 J-m/hr/m^2/°C).

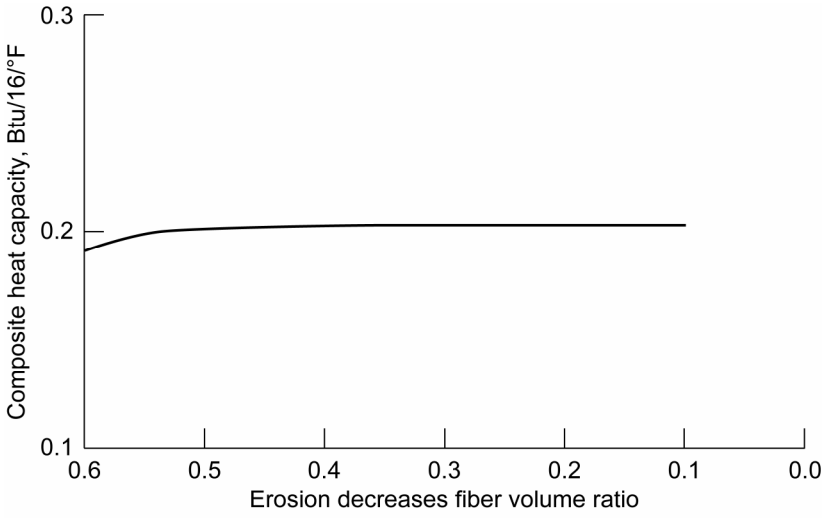

Figure 12.—Erosion effects on the composite thermal heat capacity ([0/±45/90_2/±45/0] as-graphite-fiber/intermediate modulus and strength matrix). (Btu/lb/°F = 4.19^{-3} J/kg/°C).

figure 13. Note that it approaches zero as the fiber volume ratio degrades to zero as it should since both constituents have degraded. The corresponding transverse thermal expansion coefficient is also nonlinear as shown in figure 14. However, this coefficient increases with degraded fiber volume ratio as is observed in figure 14.

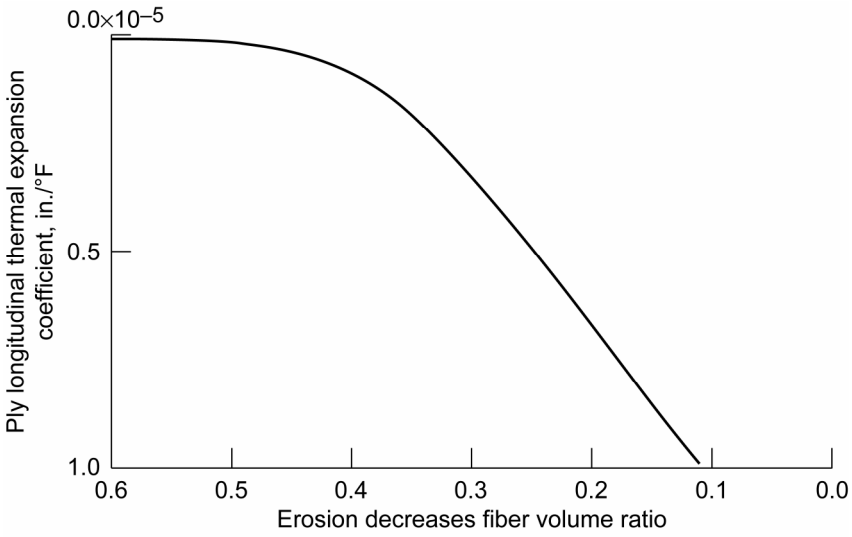

Figure 13.—Erosion degrades longitudinal thermal expansion coefficient ([0/±45/90_2/±45/0] as-graphite-fiber/intermediate modulus and strength matrix). (10^{-6}(in./in.)°F = 0.51(cm/cm)10^{-6}/°C).

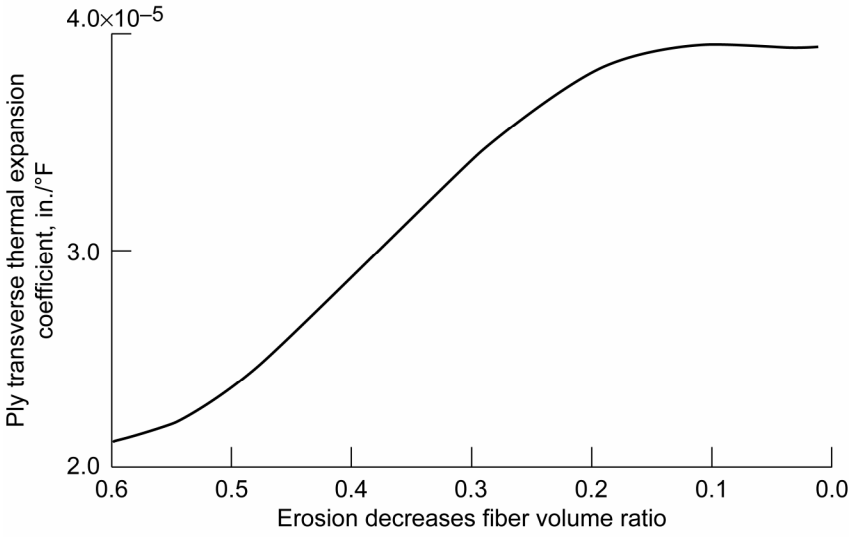

Figure 14.—Erosion effect on transverse thermal expansion coefficient ([0/±45/90_2/±45/0] as-graphite-fiber/intermediate modulus and strength matrix). (10^{-6}(in./in.)°F = 0.51(cm/cm)10^{-6}/°C).

9. Erosion Degradation on Mechanical Properties

(Moduli and Poisson's Ratios)

The equations from which these properties are evaluated are summarized in figure 15. These equations have been coded in ICAN (ref. 8). As noted in figure 15, there are six of these equations: two for normal moduli, two for shear moduli and two for Poisson's ratios. It is important to note that the void volume ratio is included as noted in the geometric properties in figure 3. The erosion effects on the ply longitudinal modulus degrades rapidly as the voids degradation increases and approaches zero as the voids approach 0.7 as can be seen in figure 16. This behavior is expected since the fiber volume ratio in that ply has completely degraded. The corresponding transverse modulus degrades rapidly nonlinearly and it too approaches zero as the voids increase to about 0.7 as is seen in figure 17. This behavior is expected also since the matrix erodes as well and the voids increase. The in-plane shear modulus erodes rapidly nonlinearly and this modulus approaches zero as the void degradation approaches 0.7 as can be observed in figure 18. The through-the-thickness shear modulus degrades equally as well as can be observed in figure 19. Note that this modulus has a lower value at the non-degraded state. The in-plane Poisson's ratio remains about unaffected of the erosion degradation as can be seen in figure 20. The through-the-thickness Poisson's ratio decreases rapidly after the void volume ratio increases beyond the 0.04 as can be seen in figure 21. This behavior is not obvious from the equation in figure 15. Note that these properties can be used to guide experimental programs in composites erosion.

Longitudinal modulus:
$$E_{\ell 11} = k_f\, E_{f11} + k_m\, E_m$$

Transverse modulus:
$$E_{\ell 22} = \frac{E_m}{1 - \sqrt{k_f}\left(1 - E_m / E_{f22}\right) =} E_{\ell 33}$$

Shear modulus:
$$G_{\ell 12} = \frac{G_m}{1 - \sqrt{k_f\left(1 - G_m / G_{f12}\right)}} = G_{\ell 13}$$

Shear modulus:
$$G_{\ell 23} = \frac{G_m}{1 - \sqrt{k_f\left(1 - G_m / G_{f23}\right)}}$$

Poisson's ratio:
$$\nu_{\ell 12} = k_f\ \nu_{f12} + k_m\ \nu_m = \nu_{\ell 13}$$

Poisson's ratio:
$$\nu_{\ell 23} = \frac{E_{\ell 22}}{2G_{\ell 23}} - 1$$

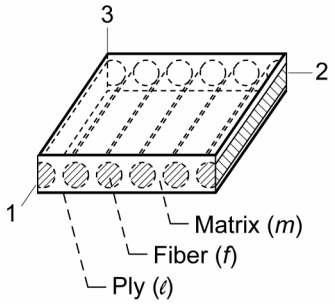

Figure 15.—Composite micromechanics, mechanical properties.

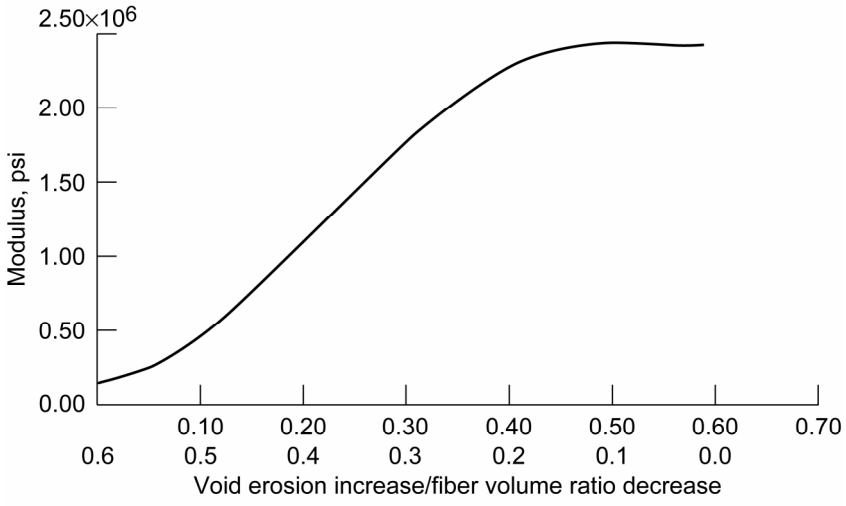

Figure 16.—Erosion effect on ply longitudinal modulus (10^6 psi = 6.89 GPa).

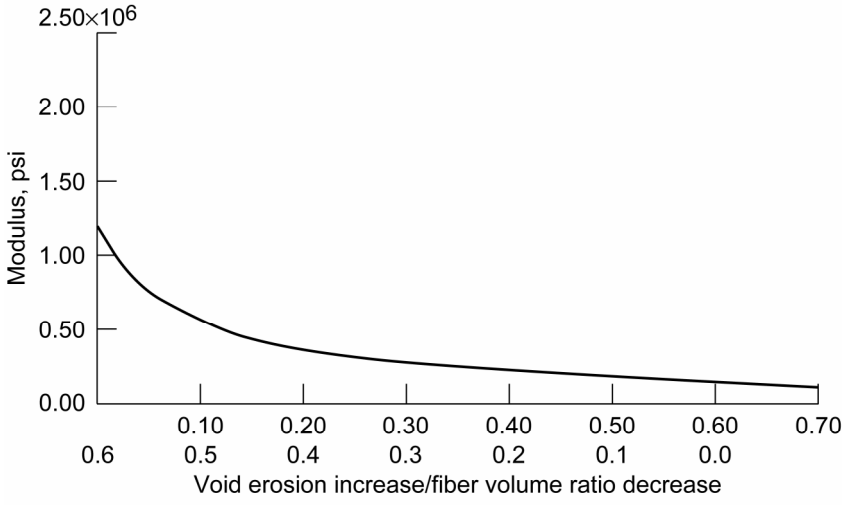

Figure 17.—Erosion effect on ply transverse modulus (10^6 psi = 6.89 GPa).

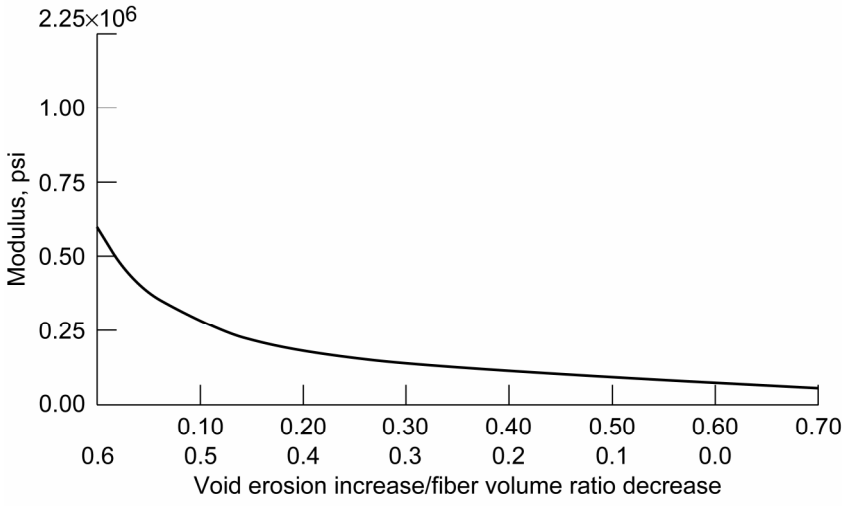

Figure 18.—Erosion effect on ply shear modulus (10^6 psi = 6.89 GPa).

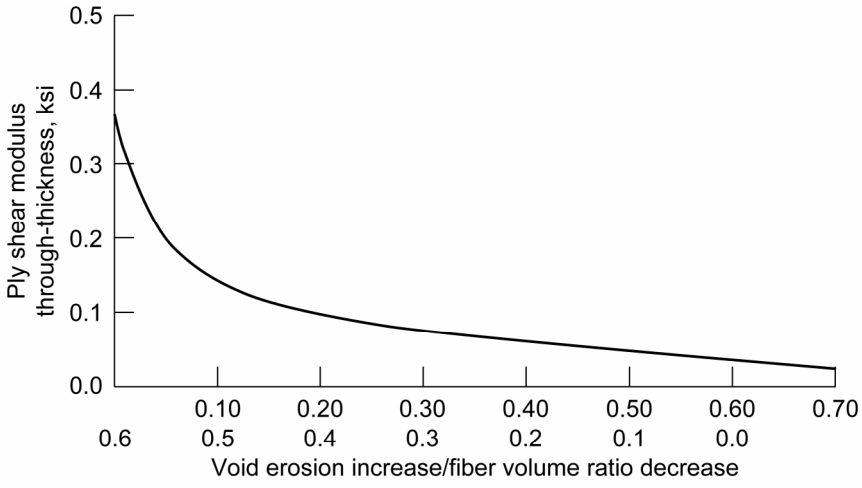

Figure 19.—Erosion effect on through-thickness shear modulus (10^6 psi = 6.89 GPa).

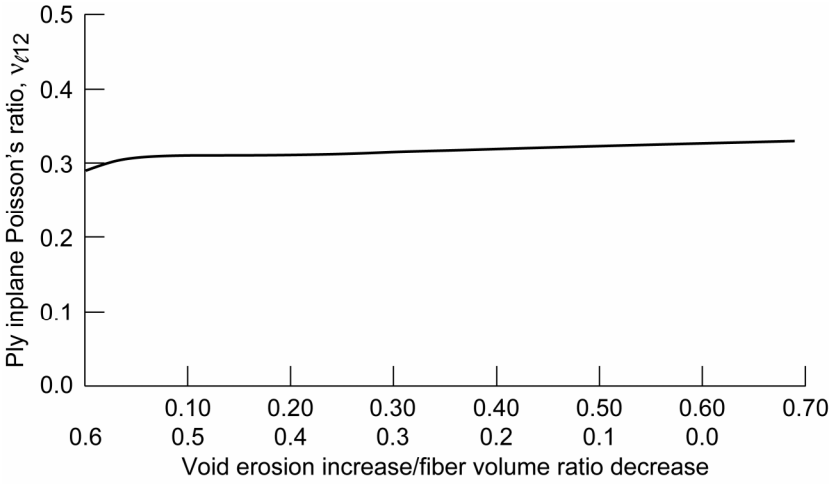

Figure 20.—Erosion effect on Poisson's ratio, $\nu_{\ell 12}$.

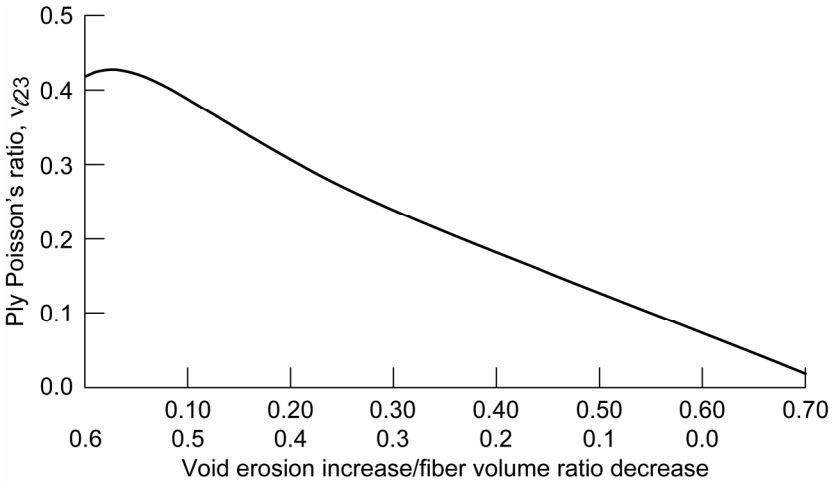

Figure 21.—Erosion effect on Poisson's ratio, $\nu_{\ell 23}$.

10. Uniaxial Strength Erosion Degradation

The equations for predicting uniaxial ply strengths with no erosion present are summarized in figure 22. These equations are coded in the ICAN composite mechanics computer code. The erosion degradation affects these strengths from the degradation in the fibers, in the matrix and the increase in the void volume ratios as described previously and is shown in figure 3. There are five of these strengths: longitudinal tension, longitudinal compression, transverse tension, transverse compression and in-plane shear. How the erosion affects these ply uniaxial strength is described below. The tensile strength degrades nonlinearly with increases in the void volume ratio and decreases in the fiber volume ratio as is shown in figure 23. The longitudinal compressive strength degrades very rapidly with increase in void volume ratio and comparable decreases in the fiber volume ratio as is shown in figure 24. The transverse tensile strength decreases nonlinearly very rapidly as the void degradation increases and the fiber volume ratio decreases as is shown in figure 25. The longitudinal transverse compressive strength decreases nonlinearly as the void volume ratio increases and the fiber volume ratio decreases as shown in figure 26. The intralaminar shear strength decreases nonlinearly as the void volume ratio in creases and the fiber

volume ratio decreases as shown in figure 27. The significance of these results is that any or all of these strengths can be used to evaluate the amount of erosion experimentally.

1. Longitudinal tension:

$$S_{\ell 11T} \approx k_f S_{fT}$$

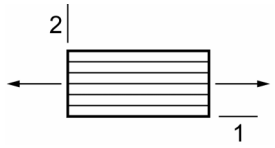

2. Longitudinal compression:

Fiber compression:

$$S_{\ell 11C} \approx k_f S_{fC}$$

Delamination/shear:

$$S_{\ell 11C} \approx 10 S_{\ell 12S} + 2.5\ S_{mT}$$

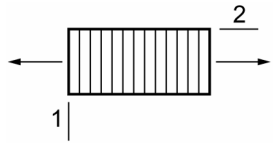

Microbuckling:

$$S_{\ell 11C} \approx \frac{G_m}{1 - k_f\left(1 - \frac{G_m}{G_{f12}}\right)}$$

3. Transverse tension:

$$S_{\ell 22T} \approx \left[1 - \left(\sqrt{k_f} - k_f\right)\left(1 - E_m / E_{f22}\right)\right] S_{mT}$$

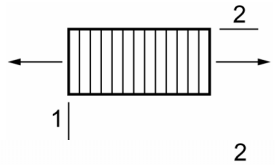

4. Transverse compression:

$$S_{\ell 22C} \approx \left[1 - \left(\sqrt{k_f} - k_f\right)\left(1 - E_m / E_{f22}\right)\right] S_{mC}$$

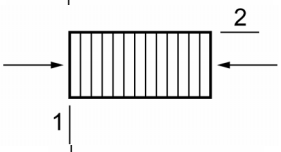

5. Intralaminar shear:

$$S_{\ell 12S} \approx \left[1 - \left(\sqrt{k_f} - k_f\right)\left(1 - G_m / G_{f12}\right)\right] S_{mS}$$

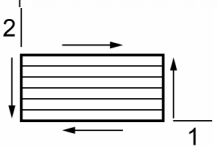

6. For voids:

$$S_m \approx \left\{1 - \left[4k_v / \left(1 - k_f\right)\pi\right]^{1/2}\right\} S_m$$

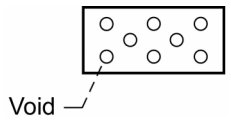

Figure 22.—Composite micromechanics, uniaxial strengths, in-plane.

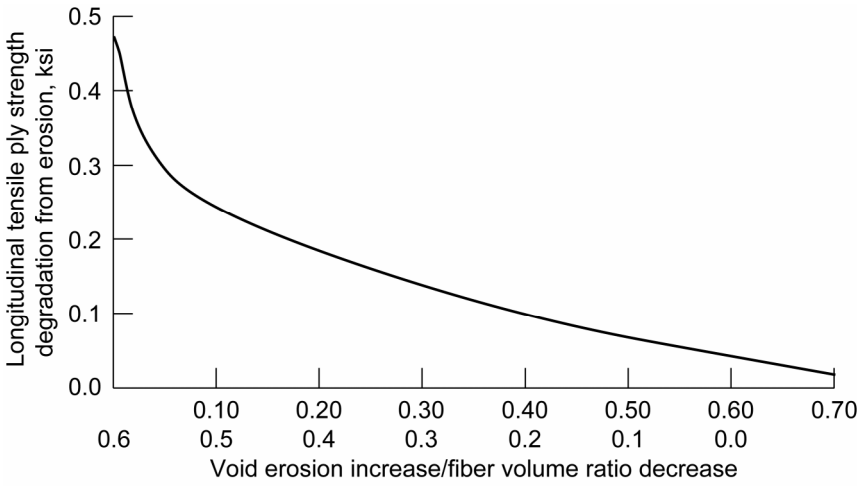

Figure 23.—Uniaxial ply strength degradation from erosion. (ksi = 6.89 MPa).

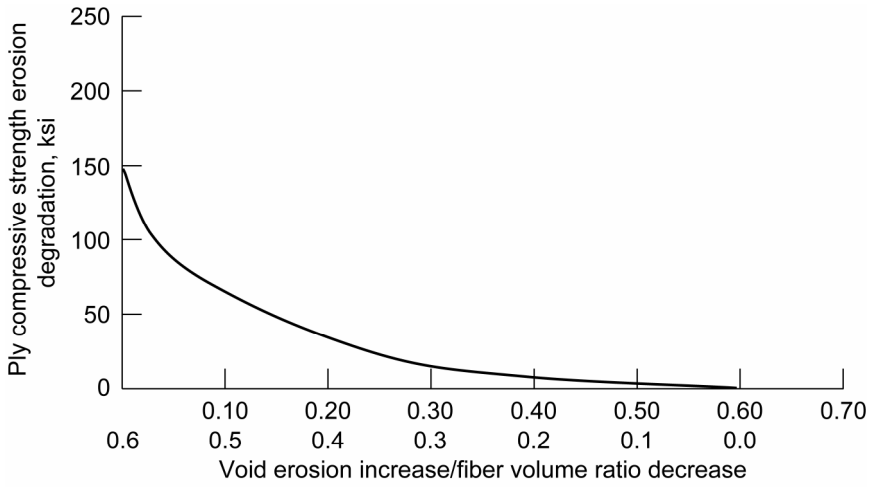

Figure 24.—Uniaxial ply compressive strength degradation from erosion. (ksi = 6.89 MPa).

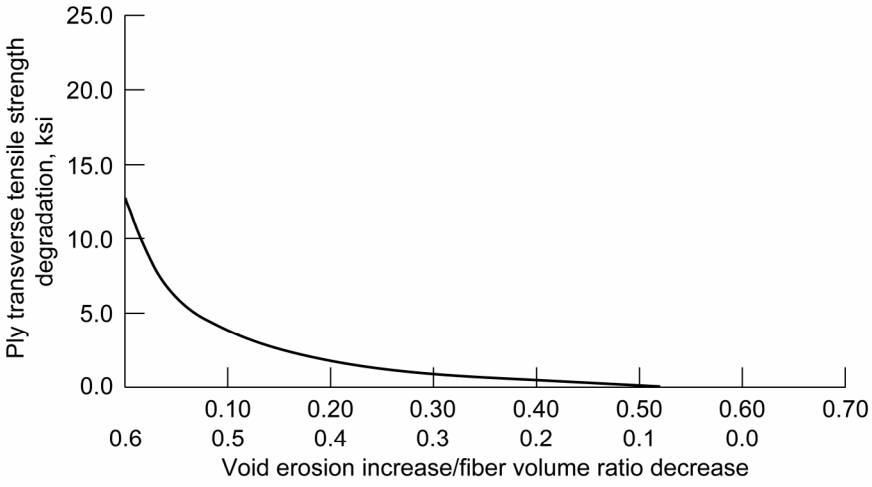

Figure 25.—Uniaxial ply transverse tensile strength degradation from erosion. (ksi = 6.89 GPa).

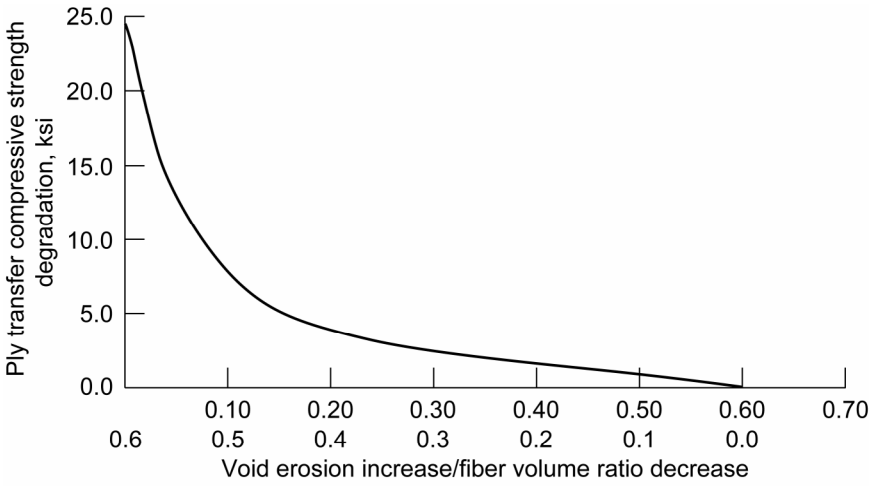

Figure 26.—Uniaxial ply transverse compressive strength degradation from erosion. (ksi = 6.89 GPa).

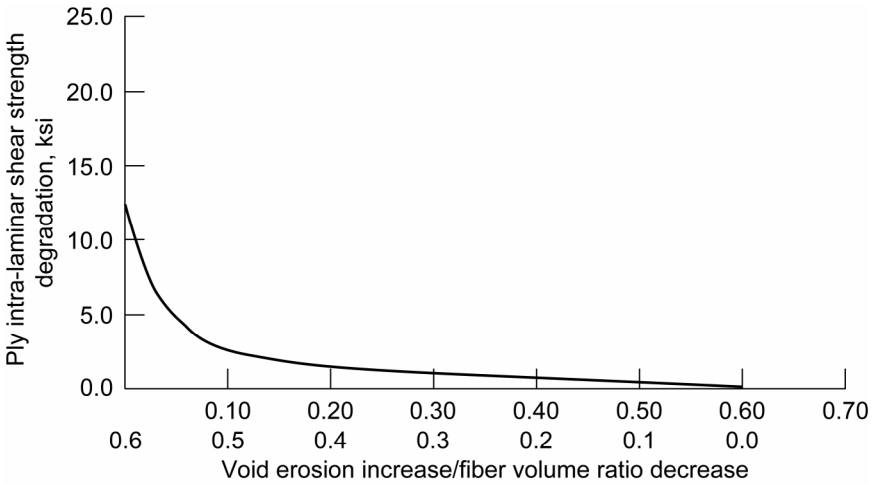

Figure 27.—Uniaxial ply intra-laminar shear strength degradation from erosion. (ksi = 6.89 GPa).

11. Erosion Effects on Laminate Strengths

The laminate strengths coded in the ICAN computer code are based on two principles, (1) when the first ply fails the laminate failed and (2) when the fibers fail in every ply in the laminate then the laminate failed. For purposes of this evaluation, only the first ply failure is appropriate because that is the only ply that will erode first. Also, these results are important because they can be used to direct experimental programs when multi angle laminates are exposed to ply erosion degradation. There are five different strengths for laminate degradation. These are axial tension, axial compression, transverse tension, transverse compression and laminate in-plane shear.

The predicted axial tensile strength of an eroded laminate is plotted versus increasing void volume ratio and decreasing fiber volume ratio in figure 28. It is observed that this strength decreases rapidly initially and near the end; it remains relatively level in the middle. The predicted laminate compressive strength is plotted in figure 29 versus increasing void volume ratio and decreasing fiber volume ratio. It is observed in figure 29 that this laminate strength degrades rapidly and nonlinearly in a continuous fashion until the void volume ratio becomes very large and the fiber volume ratio approaches zero. The laminate transverse tensile strength is plotted in figure 30 versus void volume ratio increase and fiber volume ratio decrease. This strength decreases rapidly initially and near the end but remains relatively insensitive in the middle. It exhibits the same behavior as the axial tensile strength. The laminate transverse compressive strength is plotted in figure 31 versus increasing void volume ratio and decreasing fiber volume ratio. It can be observed in figure 31 that this strength is insensitive to erosion through most of the range and decreases rapidly and nonlinearly near the end. The laminate in-plane shear strength is plotted in figure 32 versus increasing void volume ratio and decreasing fiber volume ratio. It is observed in figure 32 that this strength has unique characteristics in that it is bi-modal having both concave and convex parts. It is nonlinear throughout the region and decreases rapidly near the end. This strength will be appropriate for guiding experimental effort if the erosion is caused by shear stress predominately. This corresponds to the results in figures 2 to 4 (ref. 9) where the wear is plotted versus fiber volume ratio.

It is important to emphasize that inclusion of the eroded laminate strengths are simulated by using laminate theory combined with ply stress influence equations in addition to the equations summarized previously. These also are coded in the ICAN computer code which is truly an integrated computer code from micro mechanics to laminate theory; it also includes thermal and moisture effects. That computer code really represents a virtual composite mechanics laboratory.

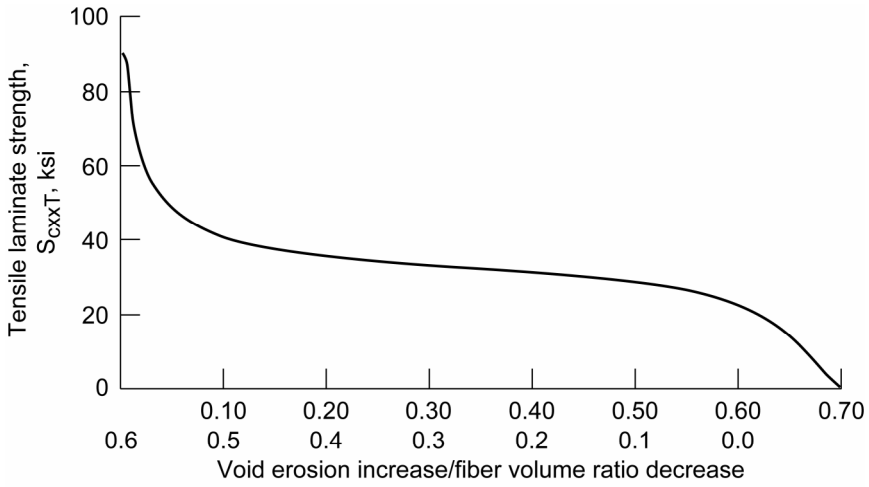

Figure 28.—Erosion effects on laminate tensile strength ([0/±45/90_2/±45/0] as-graphite-fiber/intermediate modulus and strength epoxy). (ksi = 6.89 GPa).

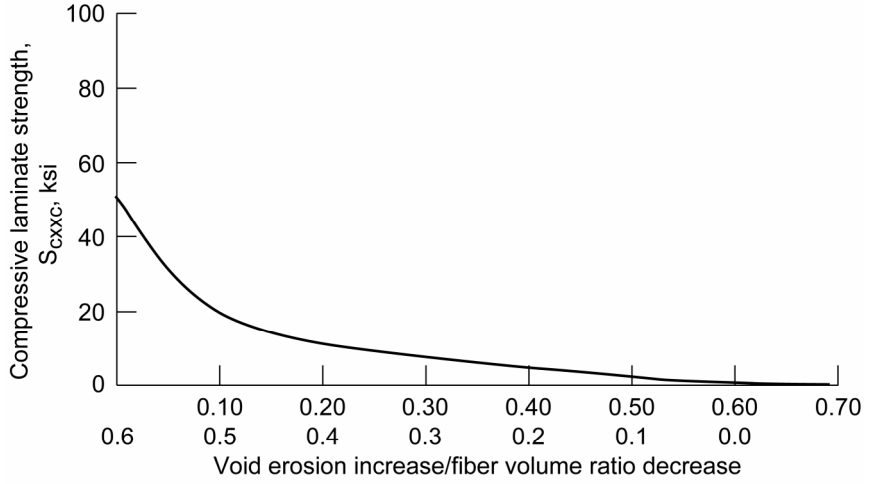

Figure 29.—Erosion effects on laminate compressive strength ([0/±45/90_2/±45/0] as-graphite-fiber/intermediate modulus and strength epoxy). (ksi = 6.89 GPa).

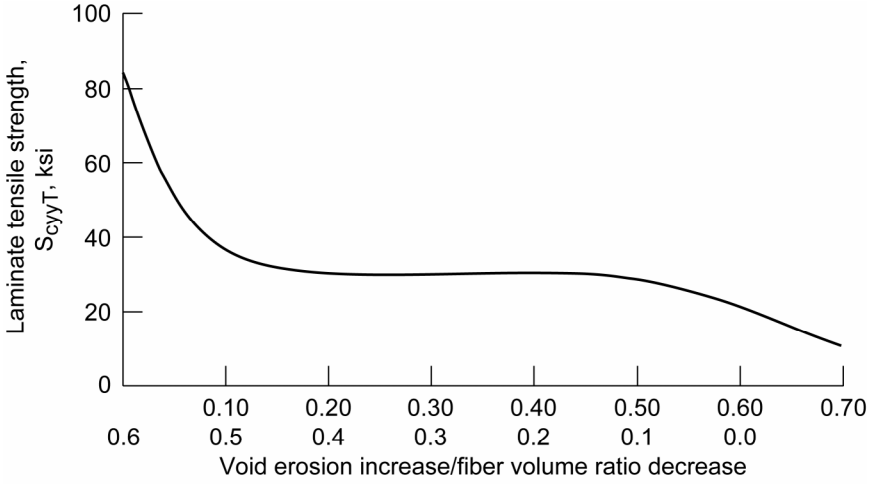

Figure 30.—Erosion effects on laminate tensile strength ([0/±45/90_2/±45/0] as-graphite-fiber/intermediate modulus and strength epoxy). (ksi = 6.89 GPa).

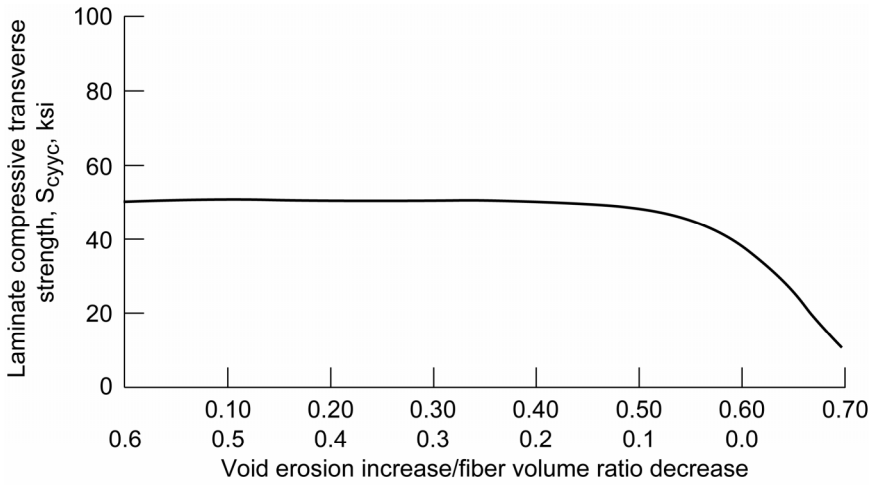

Figure 31.—Erosion effects on laminate compressive strength ([0/±45/90_2/±45/0] as-graphite-fiber/intermediate modulus and strength epoxy). (ksi = 6.89 GPa).

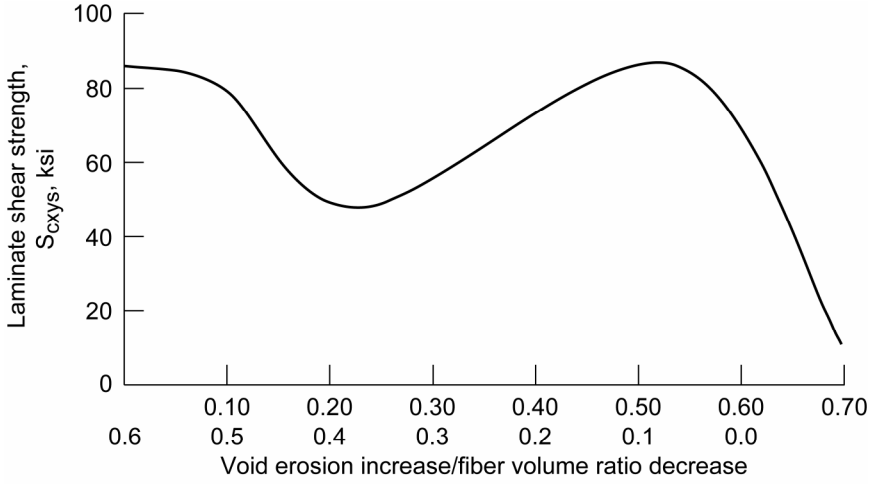

Figure 32.—Erosion effects on laminate shear strength ([0/±45/90_2/±45/0] as-graphite-fiber/intermediate modulus and strength epoxy). (ksi = 6.89 GPa).

12. Concluding Remarks

The composite erosion degradation is evaluated by two methods—the Multi Factor Interaction Model (MFIM) and by a computational simulation composites code ICAN (Integrated Composite Analyzer). Results obtained from these two methods show that:

1. The MFIM can be used to evaluate composite erosion. However, care is required to selecting the exponents and each factor ratios.
2. The ICAN evaluation is consistent with the physics of the multi scale models that are included in ICAN and can predict degradation in all the ply properties: geometric characterization, physical properties, thermal properties and mechanical properties (moduli and strengths).
3. Some of these degraded properties can be used to identify composite erosion effects and also can be used to guide experimental investigations.
4. As would be expected, the majority of the properties go to zero as the fiber and the matrix approach complete degradation.

5. The void volume ratio increases with composite degradation, as both fiber volume ratio and matrix volume ratio approach "zero" as is used in the composite erosion.
6. Computational composite mechanics is applicable when erosion occurs on a ply-per-ply basis and the eroding medium is normal to the ply.
7. The eroding medium degrades both the fiber and the matrix in the same slice through the composite thickness.
8. The friction factor is not dependent on the eroding direction but depends on the pressure exerted by the eroding medium.
9. Practically all composite properties degrade monotonically except the laminate shear strength which degrades in a bimodal fashion.

13. References

1. Klaus Friedrich, ed.: Friction and Wear of Polymer Composites, Composite Materials Series 1, Elsevier, Amsterdam, 1986.
2. Klaus Friedrich, ed.: Advances in Composite Tribology, Composite Materials Series 8 Elsevier, Amsterdam, 1993.
3. R. Reinicke, F. Haupert, and K. Friedrich, Tribology Behavior of Selected, Injection Moulded Thermoplastic Composites, Part A 29, p. 763, 1988.
4. Klaus Friedrich and Petra Reinicke, Friction and Wear of Polymer Based Composites, Mechanics of Composite Materials, Vol. 34, No. 8, p. 503, 1998.
5. M.M. Barkoula and J. Karger-Kocsis, Journal of Reinforced Plastics and Composites, Vol. 21, No. 15, p. 1377, 2002.
6. K. Friedrich, et al., Numerical and Finite Element Contact and Thermal Analysis of Real Composite-Steel Surfaces in Sliding Contact, Elsevier, p. 368, 1999.
7. N. Ohmae, J.M. Martin, and S. Mori, Micro and Nano Tribology, ASME 2005.
8. P.L.N. Murthy, C.A. Ginty, and J.G. Sanfeliz, "ICAN (Integrated Composite Analyzer)" NASA TP 3290, 1993.
9. M. Fahim, J. Indumathi, and J. Buwe, Statistical Data Analysis of Abrasive Wear Performance of Polyetherimide and Composites, Journal of Reinforced Plastics and Composites, Vol. 20, No. 12, p. 1013, 2001.

REPORT DOCUMENTATION PAGE

Form Approved
OMB No. 0704-0188

1. AGENCY USE ONLY (*Leave blank*)	2. REPORT DATE	3. REPORT TYPE AND DATES COVERED
	February 2006	Technical Memorandum

4. TITLE AND SUBTITLE

Composite Erosion by Computational Simulation

5. FUNDING NUMBERS

WBS–984754.02.07.03

6. AUTHOR(S)

Christos C. Chamis

7. PERFORMING ORGANIZATION NAME(S) AND ADDRESS(ES)

National Aeronautics and Space Administration
John H. Glenn Research Center at Lewis Field
Cleveland, Ohio 44135–3191

8. PERFORMING ORGANIZATION REPORT NUMBER

E–15300-1

9. SPONSORING/MONITORING AGENCY NAME(S) AND ADDRESS(ES)

National Aeronautics and Space Administration
Washington, DC 20546–0001

10. SPONSORING/MONITORING AGENCY REPORT NUMBER

NASA TM—2006-214096

11. SUPPLEMENTARY NOTES

Prepared for the SAMPE 2006 sponsored by the Society for the Advancement of Material and Process Engineering, Long Beach, California, April 30–May 4, 2006. Responsible person, Christos C. Chamis, organization code R, 216–433–3252.

12a. DISTRIBUTION/AVAILABILITY STATEMENT

Unclassified - Unlimited
Subject Categories: 24 and 39

Available electronically at http://gltrs.grc.nasa.gov

This publication is available from the NASA Center for AeroSpace Information, 301–621–0390.

12b. DISTRIBUTION CODE

13. ABSTRACT ***(Maximum 200 words)***

Composite degradation is evaluated by computational simulation when the erosion degradation occurs on a ply-by-ply basis and the degrading medium (device) is normal to the ply. The computational simulation is performed by a multi factor interaction model and by a multi scale and multi physics available computer code. The erosion process degrades both the fiber and the matrix simultaneously in the same slice (ply). Both the fiber volume ratio and the matrix volume ratio approach zero while the void volume ratio increases as the ply degrades. The multi factor interaction model simulates the erosion degradation, provided that the exponents and factor ratios are selected judiciously. Results obtained by the computational composite mechanics show that most composite characterization properties degrade monotonically and approach "zero" as the ply degrades completely.

14. SUBJECT TERMS

Properties degradation; Friction coefficient; Ply-by-ply removal; Nanotonic deterioration

15. NUMBER OF PAGES

28

16. PRICE CODE

17. SECURITY CLASSIFICATION OF REPORT	18. SECURITY CLASSIFICATION OF THIS PAGE	19. SECURITY CLASSIFICATION OF ABSTRACT	20. LIMITATION OF ABSTRACT
Unclassified	Unclassified	Unclassified	